Title

Early Selective Vulnerability of the CA2 Hippocampal Subfield in Primary Age-Related Tauopathy

Journal

Journal of Neuropathology & Experimental Neurology, 80(2)

ISSN

0022-3069

Authors

Walker, Jamie M
Richardson, Timothy E
Farrell, Kurt
et al.

Publication Date

2021-01-20

DOI

10.1093/jnen/nlaa153

J Neuropathol Exp Neurol
Vol. 80, No. 2, February 2021, pp. 102–111
doi: 10.1093/jnen/nlaa153

ORIGINAL ARTICLE

Early Selective Vulnerability of the CA2 Hippocampal Subfield in Primary Age-Related Tauopathy

Jamie M. Walker, MD, PhD, Timothy E. Richardson, DO, PhD, Kurt Farrell, PhD, Megan A. Iida, BS, Chan Foong, MS, Ping Shang, HT(ASCP), Johannes Attems, MD, Gai Ayalon, PhD, Thomas G. Beach, MD, PhD, Eileen H. Bigio, MD, Andrew Budson, MD, Nigel J. Cairns, PhD, María Corrada, ScD, Etty Cortes, MD, Dennis W. Dickson, MD, Peter Fischer, MD, Margaret E. Flanagan, MD, Erin Franklin, MS, Marla Gearing, PhD, Jonathan Glass, MD, Lawrence A. Hansen, MD, Vahram Haroutunian, PhD, Patrick R. Hof, MD, Lawrence Honig, MD, PhD, Claudia Kawas, MD, C. Dirk Keene, MD, PhD, Julia Kofler, MD, Gabor G. Kovacs, MD, PhD, Edward B. Lee, MD, PhD, Mirjam I. Lutz, MSc, Qinwen Mao, MD, PhD, Eliezer Masliah, MD, Ann C. McKee, MD, Corey T. McMillan, PhD, M. Marsel Mesulam, MD, Melissa Murray, PhD, Peter T. Nelson, MD, PhD, Richard Perrin, MD, PhD, Thao Pham, BS, Wayne Poon, PhD, Dushyant P. Purohit, MD, Robert A. Rissman, PhD, Kenji Sakai, MD, Mary Sano, PhD, Julie A. Schneider, MD, Thor D. Stein, MD, PhD, Andrew F. Teich, MD, PhD, John Q. Trojanowski, MD, PhD, Juan C. Troncoso, MD, Jean-Paul Vonsattel, MD, Sandra Weintraub, PhD, David A. Wolk, MD, Randall L. Woltjer, MD, PhD, Masahito Yamada, MD, PhD, Lei Yu, PhD, Charles L. White III, MD, and John F. Crary, MD, PhD

From the Department of Pathology, University of Texas Health Science Center, San Antonio, Texas, USA (JMW, TER); Glenn Biggs Institute for Alzheimer's & Neurodegenerative Diseases, University of Texas Health Science Center, San Antonio, Texas, USA (JMW, TER); Department of Pathology, State University of New York, Upstate Medical University, Syracuse, New York, USA (TER); Department of Pathology and Nash Family Neuroscience, Icahn School of Medicine at Mount Sinai, New York, New York, USA (KF, MAI, EC, PRH, DPP, JFC); Neuropathology Brain Bank & Research Core, Friedman Brain Institute, Icahn School of Medicine at Mount Sinai, New York, New York, USA (KF, MAI, PRH, JFC); Ronald M. Loeb Center for Alzheimer's Disease, Icahn School of Medicine at Mount Sinai, New York, New York, USA (KF, MAI, PRH, JFC); Department of Pathology, University of Texas Southwestern Medical Center, Dallas, Texas, USA (CF, PS, CLW); Institute for Ageing and Health, Newcastle University, Newcastle upon Tyne, United Kingdom (JA); Department of Neuroscience, Genentech Inc., South San Francisco, California, USA (GA); Neuropathology, Banner Sun Health Research Institute, Sun City, Arizona, USA (TGB); Department of Pathology, Northwestern Cognitive Neurology and Alzheimer Disease Center, Northwestern University Feinberg School of Medicine, Chicago, Illinois, USA (EHB, MEF, QM, MMM, SW); Department of Pathology, VA Medical Center & Boston University School of Medicine, Boston, Massachusetts, USA (AB, ACM, TDS); Department of Pathology and Immunology, Washington University School of Medicine, St. Louis, Missouri, USA (NJC, EF, RP); Institute for Memory Impairments and Neurological Disorders, UC Irvine, Irvine, California, USA (MC, CK, WP); Department of Neuroscience, Mayo Clinic, Jacksonville, Florida, USA (DWD, MM); Department of Laboratory Medicine and Pathobiology, University of Toronto, Laboratory Medicine Program, University Health Network, and Tanz Centre for Research in Neurodegenerative Disease, Krembil Brain Institute, Toronto, Ontario, Canada (PF, GGK); Department of Pathology and Laboratory Medicine, Emory University School of Medicine, Atlanta, Georgia, USA (MG, JG); Departments of Neurosciences and Pathology, University of California, San Diego, La Jolla, California, USA (LAH, EM, RAR); Department of Psychiatry and Alzheimer's Disease Research Center, Icahn School of Medicine at Mount Sinai, New York, New York, USA (VH, MS); Department of Neurology, Columbia University Irving Medical Center, New York, New York, USA (LH); Department of Pathology, University of Washington, Seattle, Washington, USA (CDK); Department of Pathology, University of Pittsburgh Medical Center, Pittsburgh, Pennsylvania, USA (JK); Center for Neurodegenerative Disease Research, Department of Pathology and Laboratory Medicine, Perelman School of Medicine, University of Pennsylvania, Philadelphia, Pennsylvania, USA (EBL, JQT); Institute of Neurology, Medical University of Vienna, Vienna, Austria (MIL); Department of Neurology, Perelman School of Medicine, University of Pennsylvania, Philadelphia, Pennsylvania, USA (CTM, DAW); Department of Pathology and Sanders-Brown Center on Aging, University of Kentucky, Lexington, Kentucky, USA (PTN); Department of Pathology, Oregon Health Sciences University, Portland, Oregon, USA (TP, RLW); Department of Neurology and Neurobiology of Aging, Kanazawa University Graduate School of Medical Sciences, Kanazawa, Japan (KS, MY); Departments of Pathology and Neurological Sciences, Rush University Medical Center, Chicago, Illinois, USA (JAS, LY); Department of Pathology & Cell Biology and the Taub Institute for Research on Alzheimer's Disease and the Aging Brain, Columbia University Medical Center, New York, New York, USA (AFT, J-PV); and Division of Neuropathology, Department of Pathology, Johns Hopkins University School of Medicine, Baltimore, Maryland, USA (JCT).

Send correspondence to: Jamie M. Walker, MD, PhD, Glenn Biggs Institute for Alzheimer's & Neurodegenerative Diseases, UT Health San Antonio, 7703 Floyd Curl Dr., MC 8070, San Antonio, TX 78229-3900, USA; E-mail: walkerj1@uthscsa.edu

Abstract

Primary age-related tauopathy (PART) is a neurodegenerative entity defined as Alzheimer-type neurofibrillary degeneration primarily affecting the medial temporal lobe with minimal to absent amyloid-β (Aβ) plaque deposition. The extent to which PART can be differentiated pathoanatomically from Alzheimer disease (AD) is unclear. Here, we examined the regional distribution of tau pathology in a large cohort of postmortem brains ($n = 914$). We found an early vulnerability of the CA2 subregion of the hippocampus to neurofibrillary degeneration in PART, and semiquantitative assessment of neurofibrillary degeneration in CA2 was significantly greater than in CA1 in PART. In contrast, subjects harboring intermediate-to-high AD neuropathologic change (ADNC) displayed relative sparing of CA2 until later stages of their disease course. In addition, the CA2/CA1 ratio of neurofibrillary degeneration in PART was significantly higher than in subjects with intermediate-to-high ADNC burden. Furthermore, the distribution of tau pathology in PART diverges from the Braak NFT staging system and Braak stage does not correlate with cognitive function in PART as it does in individuals with intermediate-to-high ADNC. These findings highlight the need for a better understanding of the contribution of PART to cognitive impairment and how neurofibrillary degeneration interacts with Aβ pathology in AD and PART.

Key Words: Alzheimer disease, CA2, Cognitive status, Cornu ammonis, Hippocampal subfields, Neurodegenerative disease, Primary age-related tauopathy.

INTRODUCTION

Primary age-related tauopathy (PART), previously termed tangle-only dementia, tangle-predominant senile dementia, or regarded as age-related neurofibrillary degeneration (1–3), is defined as the presence of Alzheimer-type neurofibrillary pathology in the medial temporal lobe and other structures in the absence of significant amyloid-β (Aβ) plaque deposition. In contrast and by definition, a diagnosis of Alzheimer disease (AD) neuropathologic change (ADNC) requires the presence of neurofibrillary degeneration alongside neuritic and diffuse amyloid-β (Aβ) plaques (4, 5). The Braak staging system for neurofibrillary degeneration begins with pretangles and neurofibrillary tangles (NFTs) in the locus coeruleus (termed a–c), followed by the transentorhinal and entorhinal cortex at Braak stages I–II and the hippocampal CA1 subregion at Braak stage III–IV, with neocortical neurofibrillary degeneration in Braak stages V–VI (6–9). As compared with AD (10), neurofibrillary degeneration in PART generally has a more limited distribution, with Braak stages typically ranging from I to IV. The diffuse and neuritic plaque burden ranges from Thal phase 0 to 2 and CERAD neuritic plaque score of none to sparse, but exact cutoffs are challenging to delineate (11). Many individuals above the age of 20 display some degree of tau pathology in the brainstem, principally the locus coeruleus, and almost all individuals above the age of 50 display, at minimum, neurofibrillary degeneration in the entorhinal and transentorhinal regions. However, it has also been demonstrated that over 80% of individuals in the 50–60-year age range, and at least 20% of people over the age of 80, have no amyloid plaque deposition (12). Thus, the term PART was created to describe these subjects who display NFTs without Aβ plaques. Whether older individuals with PART will develop amyloid pathology is difficult to ascertain, but Aβ plaque levels plateau in very old age (13). That is to say, despite current debate (14–16), a compelling argument can be made supporting the hypothesis that PART is a distinct neuropathologic entity, and not merely a stage along a pathologic continuum eventually leading to ADNC (4). Distinguishing neuropathological features would be helpful for further advancing our understanding of this issue.

Numerous studies have addressed the regional vulnerability of the hippocampal cornu ammonis (CA) subregions in various neurodegenerative diseases, ischemia, and epilepsy. Neurofibrillary degeneration in AD occurs earliest and is most severe in the entorhinal cortex and CA1/subiculum (9, 17–19); the CA2 subregion of the hippocampus is thought to be spared until Braak stage V in AD (6, 12). Pick disease affects the entorhinal cortex, dentate gyrus, and CA1 most severely (20), while hippocampal neurofibrillary degeneration in chronic traumatic encephalopathy (CTE) is often most severe in the CA2 and CA4 subregions (21). In addition, 4R-tauopathies, such as progressive supranuclear palsy (PSP), corticobasal degeneration (CBD), and argyrophilic grain disease (AGD), have a predilection for CA2 (19, 22). Other neurologic disorders affecting the hippocampus similarly have stereotypically affected regions: α-synuclein pathology in Lewy body disease (LBD) tends to occur earliest in the CA2 and CA3 subregions (23, 24), while neuron loss and gliosis associated with ischemia, epilepsy, and TDP-43 pathologies tend to affect select regions of the CA1 subfield (25–29).

As the next step toward understanding the neuropathologic signature of PART, we studied the hippocampal formation from 914 individuals derived from 21 different neurodegenerative disease brain banks and assessed the distribution of *p*-tau and Aβ pathology. Here, we characterize the neuropathologic and clinicopathologic differences that we observed in PART as compared with ADNC focusing on the hippocampus proper. Delineating these differences will further our understanding of the mechanisms by which individuals with PART differ from those with amyloid plaque deposition,

Funding for this work was provided by International Institutional NIH/NIA Alzheimer Disease Center grants and private grants, including: R01 NS095252, R01 AG054008, R01 AG062348, F32 AG056098, P30 AG010161, P50 AG005136, U01 AG006781, P30 AG010124, P30 AG062429, P01 AG017586, R56 AG058732, P30 AG028383, P50 AG005131, P50 AG005133, P50 AG005138, P30 AG066514, P50 AG005681, P01 AG003991, P01 AG026276, U24 NS072026, P30 AG019610, P30 AG013854, P30 NS055077, P50 AG025688, R01 AG021055, P50 AG016573, P50 AG008702, P30 AG08017, the Alzheimer's Association (NIRG-15-363188), the Rainwater Charitable Foundation (Tau Consortium), David and Elsie Werber, J.M.R. Barker Foundation, The McCune Foundation, and the Winspear Family Center for Research on the Neuropathology of Alzheimer Disease, Knight Alzheimer Disease Research Center, The Arizona Department of Health Services, and the Michael J. Fox Foundation for Parkinson's Research.

The authors have no duality or conflicts of interest to declare.

Supplementary Data can be found at http://academic.oup.com/jnen.

TABLE. Overview of Demographic, Clinical, and Pathologic Features

Braak Stage	n	CERAD NP Score		Thal Phase			Diagnosis				Age Range, Years (Average)	Cognitive Status*		
		None	Sparse+	0	1–2	3+	Definite PART	Possible PART	ADNC	Other		Normal	MCI	Dementia
0–I	152	151	1	99	46	7	83	36	6	27	51–98 (75.6)	66	18	7
II	102	99	3	62	35	5	62	35	4	1	55–102 (78.8)	19	9	6
III	295	287	8	167	108	20	167	108	16	4	57–108 (86.4)	106	35	44
IV	348	299	49	172	148	28	172	148	27	1	53–107 (89.9)	87	19	30
V+	17	9	8	3	2	12	2	2	12	1	84–95 (88.9)	3	1	10

*Clinical data not available for all cases.

and how the presence of plaques may promote a more widespread distribution of neurofibrillary degeneration.

MATERIALS AND METHODS

Ethics Approval and Consent to Participate

This study was conducted in accordance with the declaration of Helsinki and was performed with IRB approval at all applicable institutions.

Patient Samples

Autopsy case material was derived from 21 institutions: Banner Sun Health Research Institute, Boston University School of Medicine, Columbia University Irving Medical Center, Emory Healthcare, Johns Hopkins Medical Center, Massachusetts General Hospital, Mayo Clinic, Medical University of Vienna, Mount Sinai Medical Center, Newcastle Medical Centre, Northwestern Medical Center, Oregon Health & Sciences University, Rush University Medical Center, University of California, Irvine Medical Center, University of California, San Diego Medical Center, University of Kentucky HealthCare, University of Pennsylvania Health System, University of Pittsburgh Medical Center, University of Texas Southwestern Medical Center, University of Washington Medical Center, and Washington University in St. Louis. The clinical inclusion and exclusion criteria include age ≥50 years and absence of motor neuron disease (MND), movement disorders, or frontotemporal dementia (FTD). Neuropathologic inclusion criteria include Braak stage 0–VI, absent or sparse neuritic plaques by CERAD criteria, and absence of other tauopathies (Supplementary Data Table S1).

A total of 914 cases were included for preparation of histologic and immunohistochemical stains with the subsequent generation of whole slide images using an Aperio scanner at The University of Texas Southwestern Medical Center, Dallas, Texas. Unstained slides from the hippocampus (level 7) (30) and middle frontal gyrus (4-µm-thick sections from formalin-fixed, paraffin-embedded blocks) were requested. Unstained sections designated as hippocampus were received for 1013 cases. Corresponding unstained frontal sections were received for 476 cases. A total of 99 cases were considered inadequate for diagnosis (due to torn tissue, wrong section or wrong level of the hippocampus). These cases were excluded from all analyses. Clinical cognitive data, such as Clinical Dementia Rating (CDR) and Mini-Mental State Examination (MMSE) scores, were available for 279 and 250 cases, respectively. The age, Braak stage (6), CERAD neuritic plaque score (31), Thal phase (32), neuropathologic diagnosis and cognitive status (if available) for the study subjects are outlined in the Table.

Neuropathological Analyses

Comprehensive histopathological workups were performed as per the protocols of the respective brain banks. Additional staged assessments were performed at UT Southwestern Medical Center, including Luxol fast blue/hematoxylin & eosin (LFB/H&E), Hirano modified Bielschowsky silver stain, and phospho-tau (*p*-tau) immunohistochemistry (IHC) (AT8; MN1020, Thermo Fisher Scientific, Waltham, MA). One hippocampal and one frontal section from each case were stained with LFB/H&E. In addition, hippocampal sections from each case were immunostained for *p*-tau. Frontal sections were stained with Hirano silver stain and β-amyloid IHC (6E10; SIG-39320, Covance, Inc., Princeton, NJ) on a Leica Bond III automated stainer, according to the manufacturer's protocols (Leica Microsystems, Buffalo Grove, IL). If a case was immunopositive for β-amyloid in the frontal neocortex, then β-amyloid IHC was subsequently performed on the hippocampal section to determine the Thal phase and *p*-tau IHC was performed on the frontal section to assess possible neuritic plaque burden. In addition, hippocampal sections from a subset of cases with prominent CA2 neurofibrillary degeneration were immunostained for 3R-tau (RD3; 05-803, EMD Millipore Corporation, Temecula, CA) and 4R-tau (ET3, gift of Dr. Peter Davies). Stained sections were scanned on an Aperio CS2 ScanScope whole slide scanner (Leica Microsystems).

Histopathological Assessments and Semiquantitative Analysis

All cases were analyzed using Aperio ImageScope (version 12.3) software (Leica Microsystems). Scoring was performed by 2 board-certified neuropathologists familiar with neurodegenerative disorders (J.M.W. and T.E.R.). An estimated Thal phase was assigned using frontal and/or hippocampal β-amyloid immunostained sections: Thal 0 = complete absence of β-amyloid-immunoreactive plaques; Thal 1 = any parenchymal β-amyloid plaques in the frontal

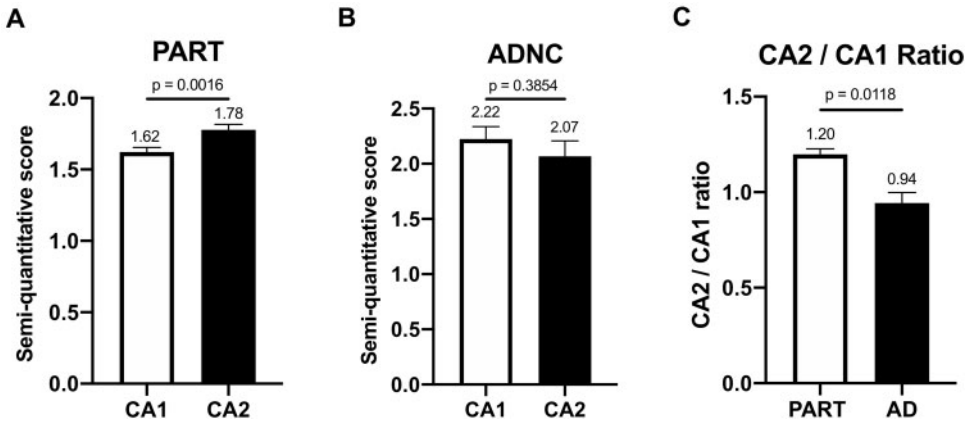

FIGURE 1. Differential hyperphosphorylated tau (*p*-tau) burden in primary age-related tauopathy (PART) versus Alzheimer disease neuropathologic change (ADNC). **(A)** Semiquantitative scores for neurofibrillary degeneration in CA1 and CA2 in PART by *p*-tau (AT8) immunostaining, demonstrating a significantly higher level of neurofibrillary degeneration in CA2 compared with CA1 ($p = 0.0016$). **(B)** Semiquantitative scores in subjects with ADNC, demonstrating no significant difference between CA1 and CA2 subregions ($p = 0.3854$), unlike PART. **(C)** Ratio of CA2 to CA1 neurofibrillary degeneration by semiquantitative AT8 analysis in PART ($n = 720$) and ADNC ($n = 57$), demonstrating a significantly higher CA2/CA1 ratio in PART compared with ADNC ($p = 0.0118$).

neocortex only; Thal 2 = any parenchymal β-amyloid plaques in the frontal neocortex as well as the transentorhinal/entorhinal cortex or CA1 subregion of the hippocampus; Thal 3 = any parenchymal β-amyloid plaques in the frontal neocortex, transentorhinal/entorhinal or CA1 subregion, and the molecular layer of the dentate gyrus; and Thal 4 = any parenchymal β-amyloid plaques in the frontal neocortex, transentorhinal/entorhinal or CA1 subregion, and CA4 subregion of the hippocampus, as previously reported (32). CERAD neuritic plaque scores were estimated based on the density of neuritic plaques on the Hirano silver stain in the frontal neocortex, as previously reported (31). Cases with a Thal phase of 0 and CERAD neuritic plaque score of none were defined as definite PART, while cases with a Thal phase of 1–2 (or CERAD neuritic plaque score of sparse) were defined as possible PART as per published consensus criteria (11). Furthermore, cases that qualified as intermediate or high ADNC based on the NIA-AA Reagan criteria (5) were defined as such. From the 914 cases in the cohort, 486 cases were designated as definite PART, 329 cases were designated as possible PART, 28 cases displayed minimal neuropathologic changes, 6 were neither PART nor ADNC (for example, PSP and GGT), and 65 were designated as ADNC or were on the AD continuum (for example, cases with Braak stage I or II, but Thal phase of $\geq$3 were placed in the ADNC category). Supplementary Data Figure S1 demonstrates an overview of the diagnostic categories and distribution of the 1013 cases that were received for analysis.

Hyperphosphorylated tau (*p*-tau, AT8) IHC stains of the hippocampal and frontal sections were evaluated for each case to reassess *p*-tau burden and Braak stage (Supplementary Data Fig. S2) (6). A minority of cases with NFTs in the frontal neocortical sections were given a Braak score of at least V, as the primary visual and auditory cortex were unavailable for rereview. Neurofibrillary degeneration in all hippocampal subregions (CA1–CA4) (Supplementary Data Fig. S3) (26, 33), the entorhinal cortex, and dentate gyrus were given semiquantitative scores of severe = 3, moderate = 2, mild = 1, rare to sparse = 0.5, or none = 0 (Supplementary Data Fig. S4).

Statistical Analysis

A Student *t*-test (unpaired) was utilized to assess statistical significance in the difference of *p*-tau burden in the CA1 and CA2 subregions of the hippocampus. Differences in the *p*-tau burden present in all hippocampal subregions were calculated using analysis of variance (ANOVA). ANOVA and Student *t*-tests were utilized for statistical analyses of the relationship between Thal phase, neuritic plaque score and CA2/CA1 ratio. Clinical correlations with Braak stage were calculated using linear regression. All statistical analyses were calculated using GraphPad Prism version 8.4 (GraphPad, La Jolla, CA).

RESULTS

Hippocampal Subregion Distribution of Neurofibrillary Degeneration in PART

Semiquantitative analysis of the AT8-immunostained hippocampi revealed that neurofibrillary degeneration in PART was significantly greater in the CA2 subregion of the hippocampus than in CA1 ($p = 0.0001$, Fig. 1A), unlike ADNC in which no significant difference between CA1 and CA2 neurofibrillary degeneration was observed ($p = 0.3854$, Fig. 1B). We also found that the CA2/CA1 ratios of neurofibrillary degeneration in the PART cases were significantly higher than in the ADNC cases ($p = 0.0118$, Figs. 1C, 2, and 3). This subregion distribution trend was previously presented as preliminary data (34) prior to analyzing the full cohort. Subsequently, other studies reported similar neuropathologic changes in smaller independent PART cohorts (35, 36).

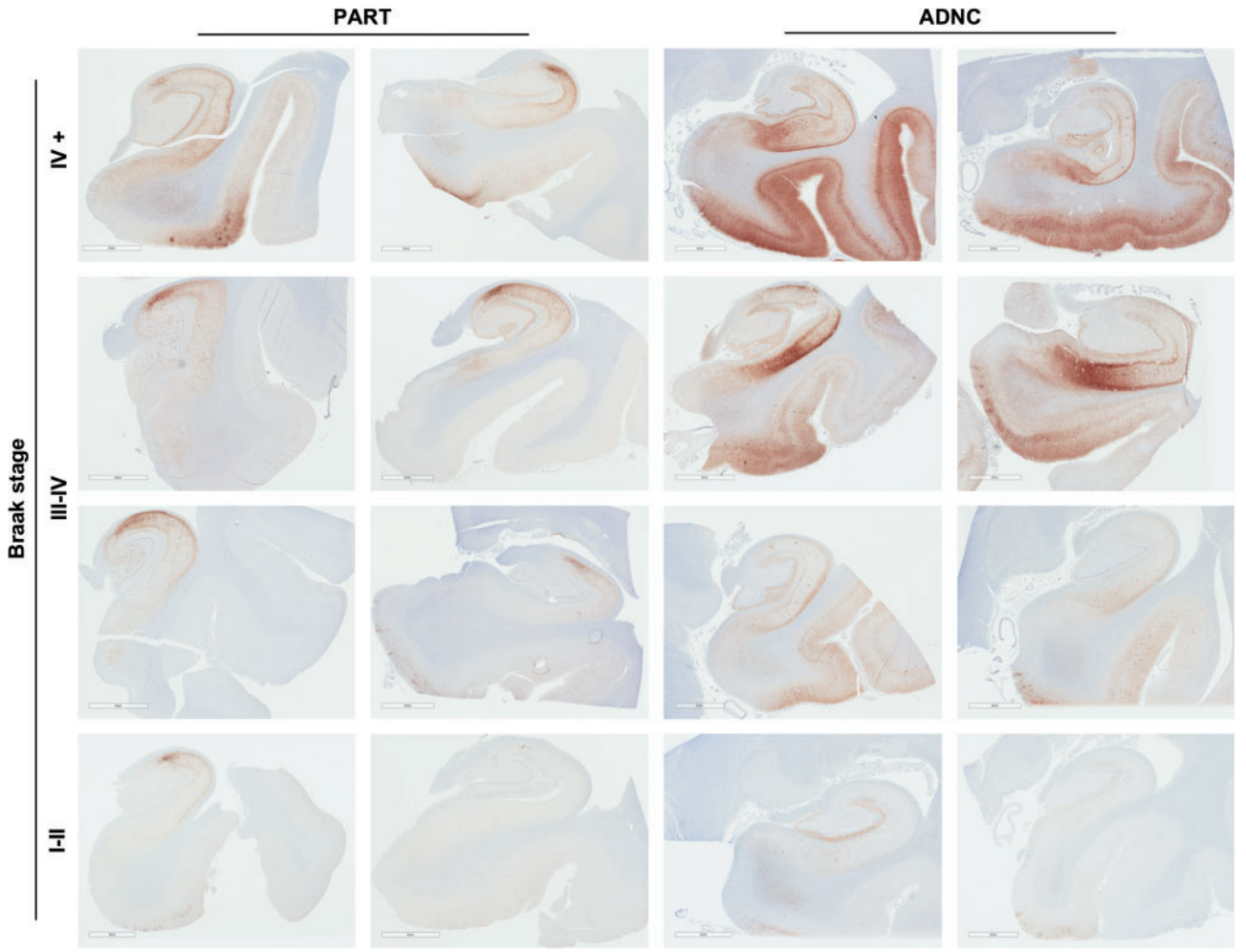

FIGURE 2. Examples of hyperphosphorylated tau (*p*-tau, AT8) immunostaining in hippocampi in primary age-related tauopathy (PART) and Alzheimer disease neuropathologic change (ADNC). There is an early predilection for CA2 pathology in PART with relative sparing of the entorhinal and CA1 regions, and sparing of CA2 in ADNC with more dense neurofibrillary degeneration in CA1 and the entorhinal regions. All scale bars = 4 mm.

Analysis of CA2 Neurofibrillary Degeneration in PART

Many 4R-tauopathies, such as CBD, PSP, and AGD, similarly display a selective vulnerability of the CA2 subregion of the hippocampus for neurofibrillary degeneration (22). It is known that PART harbors 3R/4R+ Alzheimer-type NFTs (11). However, the predilection for CA2 raised the question of whether the tangles present in CA2 in PART are the usual 3R/4R+ Alzheimer-type NFTs or solely 4R-tau-immunopositive tangles. With 3R-tau and 4R-tau immunostains, we confirmed that PART CA2 NFTs are both 3R+ and 4R+ (Fig. 4). Thus, they represent 3R/4R+ Alzheimer-type NFTs in a non-Alzheimer-type distribution. This also demonstrated that the PART CA2 tangles are distinct from the 4R+ pretangles that are observed in AGD.

Analysis of Entorhinal Cortex and All Subregions of the Hippocampus in PART and ADNC

Semiquantitative scoring of neurofibrillary degeneration was performed on the entorhinal cortex, subiculum/CA1, CA2, CA3, CA4, and dentate gyrus. There were significant differences identified between all analyzed subregions in definite and possible PART groups (Fig. 5A, B), however, the only difference found in the ADNC cases was between the entorhinal/CA1/CA2 and CA3/CA4/dentate regions (Fig. 5C). Significant differences were found in every subregion between our ADNC cases and the possible and definite PART groups, with the exception of CA2, in which no significant difference was observed when comparing any group (Fig. 5D). That is to say, all subregions of ADNC cases have higher scores than PART, except the CA2 subregion. The mean CA2 score in ADNC cases is not significantly different from the mean CA2 score in PART, although the trend appears to be higher in ADNC cases. This is most likely because the overall average Braak stage for the ADNC cases is higher than that of the PART cases (Supplementary Data Fig. S2). CA2 neurofibrillary degeneration is present in PART as an early finding, without corresponding elevation of NFT pathology in the entorhinal or CA1 subregions, as is observed in ADNC. In fact, 73 PART cases displayed absent or sparse neurofibrillary

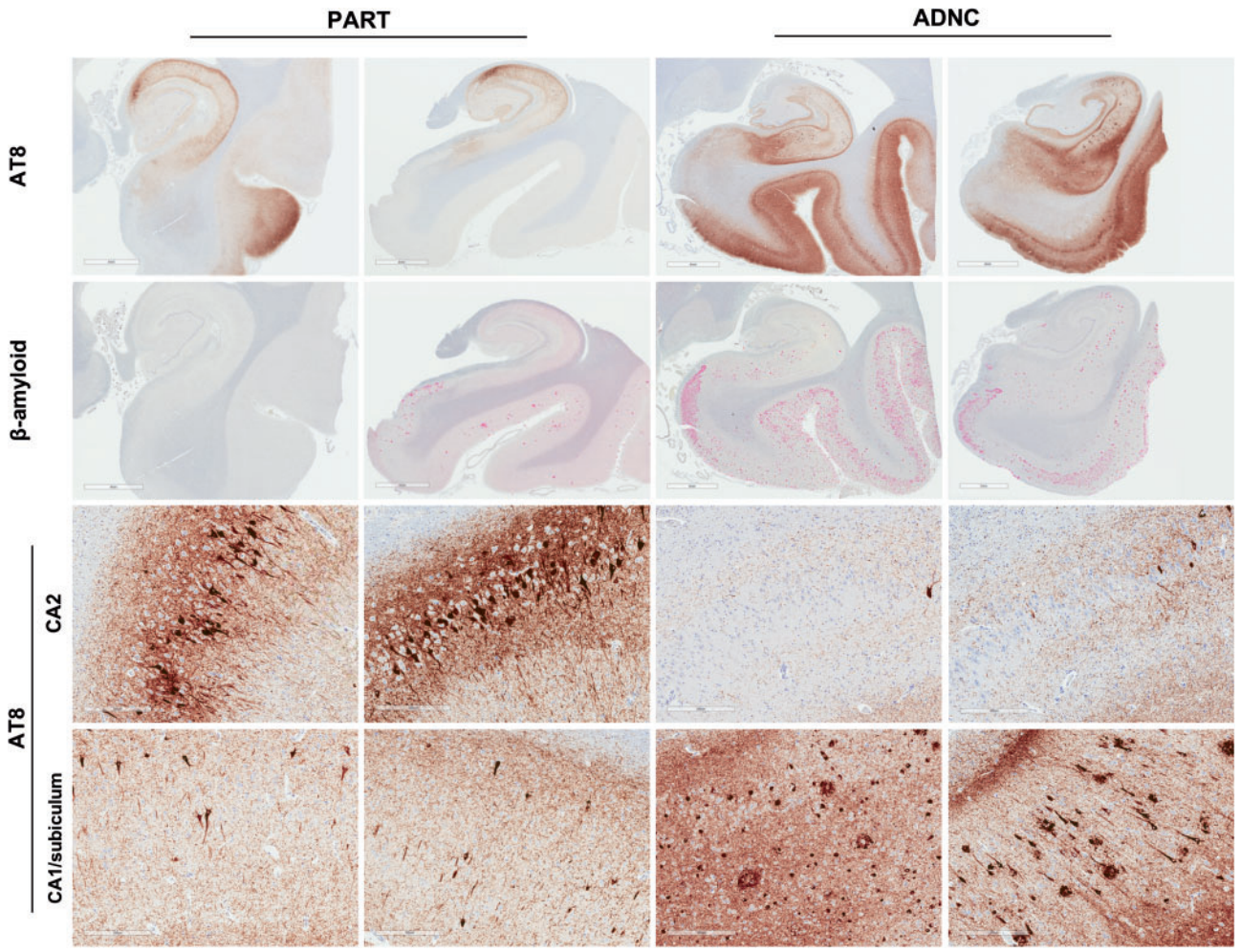

FIGURE 3. Examples of representative hippocampal sections from subjects with primary age-related tauopathy (PART) and Alzheimer disease neuropathologic change (ADNC) demonstrating AT8 and β-amyloid immunostaining patterns. Higher power images of the CA2 and CA1/subiculum subregions demonstrate significantly more neurofibrillary degeneration in the CA2 subregions of PART compared with ADNC, and significantly more neurofibrillary degeneration in the CA1/subiculum subregions of ADNC compared with PART. Scale bars in top 8 panels = 4 mm; scale bars in bottom 8 panels = 300 μm.

degeneration in the entorhinal cortex with a corresponding CA2 score of ≥1, whereas only 1 ADNC case displayed this pattern.

Relationship of Thal Phase and CA2/CA1 Ratio

For this analysis, cases were separated into subgroups based on Thal phase. Significant differences were identified in the CA2/CA1 ratio in all subgroups with decreasing CA2/CA1 ratio as Thal phase increases (Fig. 6A). In the Thal phase 3 subgroup (n = 30), there were 5 cases without neuritic plaques in the hippocampus or frontal neocortex. Four out of 5 cases were clinically categorized as "normal." The other case was a 101-year-old individual given a clinical diagnosis of AD. On our examination, this individual had Braak stage IV with severe aging-related tau astrogliopathy (ARTAG). The average CA2/CA1 ratio in the Thal phase 3 cases without neuritic plaques was 2.13, whereas the average CA2/CA1 ratio in the Thal phase 3 cases with neuritic plaques was 0.95 ($p = 0.001$, Fig. 6B). Cognitive status did not correlate in these subgroups. However, one would expect that cases without neuritic plaques and with higher CA2/CA1 ratio would have significantly better cognition. Thus, Thal phase 3 cases lie on a border where they could represent AD-related or PART pathology with significant CA2 neurofibrillary degeneration and a higher CA2/CA1 ratio. In addition, the Thal phase 3 cases with the high CA2/CA1 ratio were less cognitively impaired based on clinical diagnoses.

Clinicopathologic Correlations of NFD in PART and ADNC

While Braak stage had a significant positive correlation with cognitive function in cases with ADNC in terms of CDR

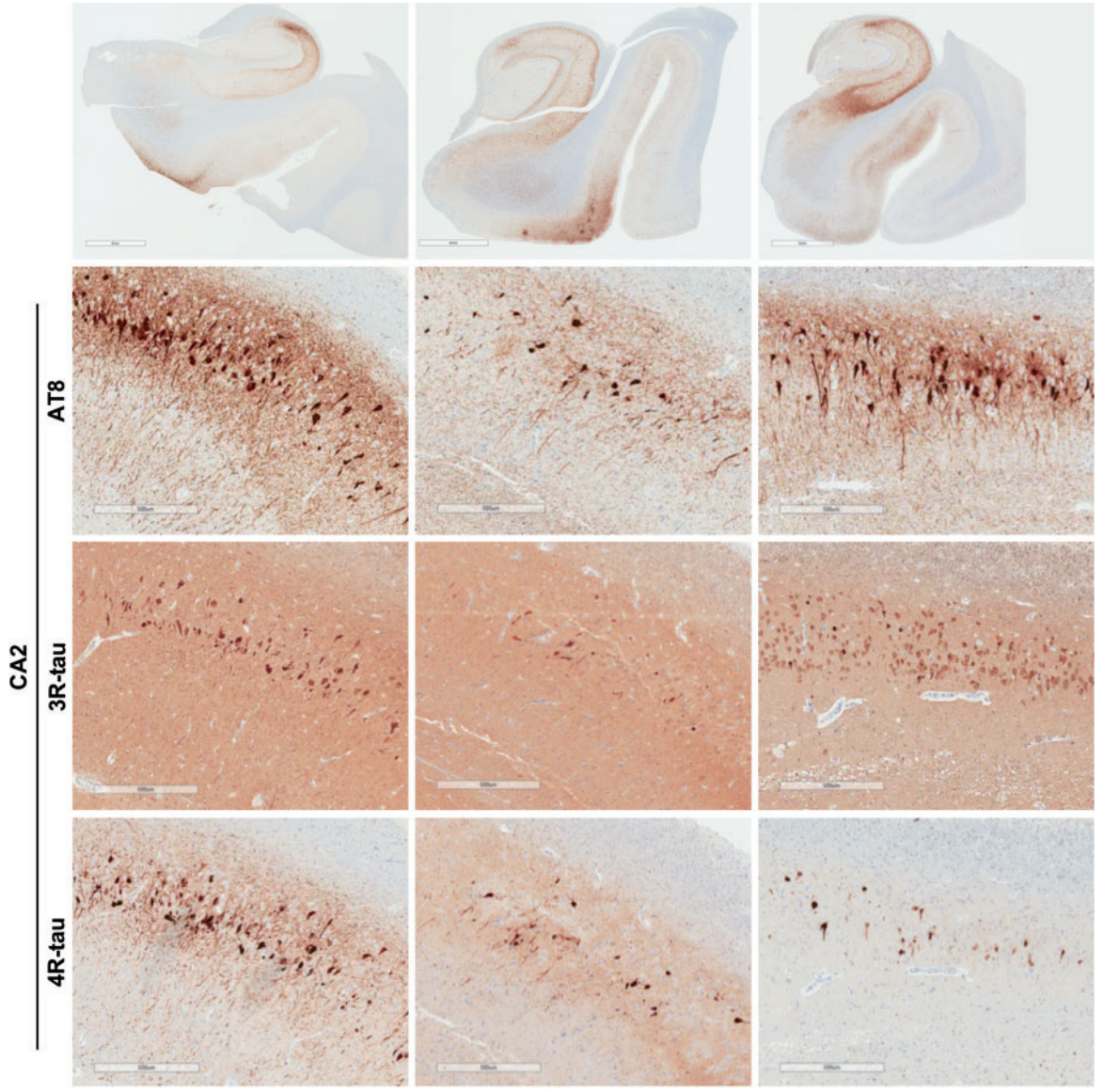

FIGURE 4. Tau isoform expression in the CA2 subregion in PART. **(A–C)** Low power of hippocampi from 3 AT8-immunostained PART, as well as high-power images of the CA2 subregions with AT8 **(D–F)**, 3R-tau **(G–I)**, and 4R-tau immunostaining **(H–J)**. PART brains display both 3R and 4R-tau isoforms, unlike 4R-tauopathies that may demonstrate CA2 selective AT8-immunopositive lesions, such as PSP, CBD, and AGD. Scale bars in top 3 panels = 4 mm; scale bars in bottom 9 panels = 500 μm.

($r = 0.66$; $p = 0.0057$), Braak stage did not correlate with CDR in PART ($r = 0.10$; $p = 0.1249$) (Fig. 7A). In addition, there was a significant inverse correlation between Braak stage and MMSE scores in ADNC cases ($r = -0.53$; $p = 0.0224$), whereas there was no correlation between Braak stage and MMSE in PART ($r = -0.01$; $p = 0.8441$) (Fig. 7B).

DISCUSSION

In this report, we demonstrate significant differences in the hippocampal distribution of neurofibrillary degeneration in PART compared with AD. The distribution of NFTs in PART does not follow the typical Braak staging system. Instead, NFTs demonstrate a predilection to affect the CA2 subregion of the hippocampus before the entorhinal cortex and the CA1 subregion in PART (Figs. 2 and 3) and demonstrates a significantly higher CA2/CA1 ratio of neurofibrillary degeneration compared with ADNC (Fig. 1C). This selective vulnerability of CA2 is similar to 4R-tauopathies, however the NFTs in PART are 3R/4R+ Alzheimer-type NFTs (Fig. 4). It is possible that the lack of abundant plaques may drive this altered distribution of neurofibrillary degeneration (4). Consistent with this hypothesis, there was a trend in this cohort for the CA2/CA1 ratio to increase with lower Thal phase (Fig. 6). It would be interesting to expand this analysis with more ADNC cases, to more fully understand the spectrum of

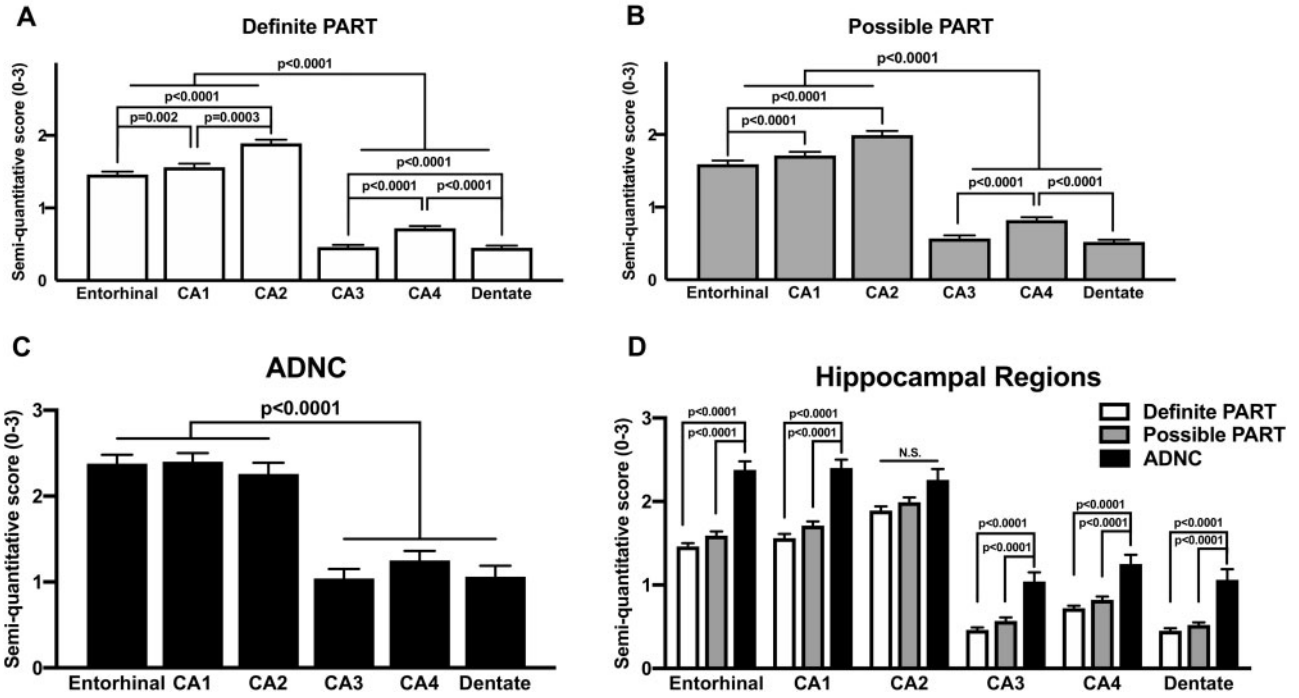

FIGURE 5. Selective vulnerability of hippocampal subregions in primary age-related tauopathy (PART) compared with Alzheimer disease neuropathologic change (ADNC). Semiquantitative scores for tau in each hippocampal subregion (entorhinal cortex, CA1–4, dentate gyrus) in **(A)** definite PART (n = 486), demonstrating significant differences between all measured regions, **(B)** possible PART (n = 329), demonstrating varying significant differences between entorhinal, CA1, CA2, CA3, CA4, and dentate regions, and **(C)** ADNC (n = 65), demonstrating significant differences between the entorhinal/CA1/CA2 and CA3/CA4/dentate regions. In addition, there are significant differences in semiquantitative scores between ADNC and both definite and possible PART in the entorhinal, CA1, CA3, CA4, and dentate regions without significant differences in the CA2 subregion between any subgroup **(D).**

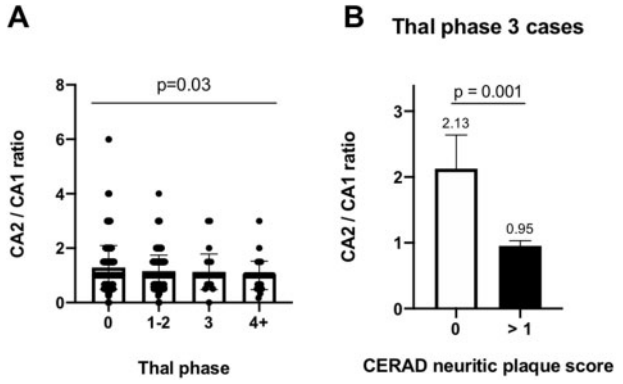

FIGURE 6. Thal phase is inversely correlated with CA2/CA1 *p*-tau burden ratio. **(A)** There is a significant progression toward higher CA2/CA1 ratio with lower Thal phase (p = 0.034). **(B)** There is a significantly higher CA2/CA1 ratio in Thal phase 3 cases with no neuritic plaques in the hippocampus or neocortex as compared with Thal phase 3 cases with CERAD ≥1 (p = 0.0011).

amyloid-associated tau changes. We also think that individuals with intermediate amyloid pathology (i.e. Thal phase 3) could represent an intermediate state that may display ADNC or PART-like distribution (with a predilection for CA2), and individuals with PART-like pathology may have a significantly milder disease.

CA2 NFTs are also observed in CTE, another mixed 3R/4R tauopathy (21). In CTE, this change is often found in combination with CA4 neurofibrillary degeneration, and these cases often have a low amyloid burden. These cases with CA2/CA4 neurofibrillary degeneration may represent CTE superimposed on PART; however, CTE could be an entirely separate entity that displays a predilection for CA2 and CA4 on its own given the young age of many reported participants with CTE and hippocampal tau pathology (29). It is also known that LBD involves selective vulnerability of the CA2-3 subregions of the hippocampus for α-synuclein-immunoreactive Lewy bodies and Lewy neurites (23, 24). However, the amount of CA1 pathology in cases of LBD correlates better with cognitive function than the amount of CA2 pathology (37, 38).

Previous studies comparing PART and AD have demonstrated less overall cognitive impairment and less steep rates of decline in PART patients, as well as a later onset of disease symptoms (39). In the current study, we found that unlike AD, there is no significant correlation between Braak stage and cognitive function in PART (Fig. 7). The reasons for this are unclear; however, this is consistent with PART being a more benign aging phenomenon. It is also possible that there are more resilient individuals within the PART cohort. An

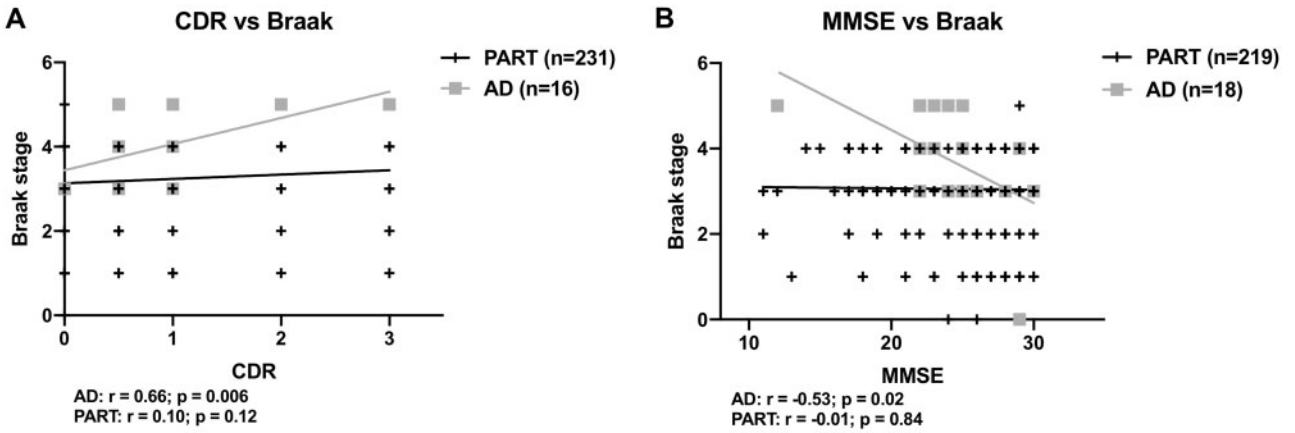

FIGURE 7. Braak stage does not correlate with cognitive impairment in primary age-related tauopathy. **(A)** Correlation between Braak stage and CDR in ADNC (n = 16) and PART (n = 231) cases with available CDR data. There is a significant positive correlation between Braak stage and CDR in ADNC ($r = 0.66$; $p = 0.0057$), but no association in PART ($r = 0.10$; $p = 0.1249$). **(B)** Correlation between Braak stage and MMSE in ADNC (n = 18) and PART (n = 219). MMSE scores are inversely correlated with Braak stage in ADNC cases ($r = –0.53$; $p = 0.0224$), but there is no correlation between Braak stage and MMSE scores in PART cases ($r = –0.01$; $p = 0.8441$).

alternative hypothesis is that the cognitive tests currently used do not adequately assess the functionality of the regions most severely involved in PART, such as CA2. Studies have demonstrated that CA2 may be involved in social memory (40, 41). This has mostly been shown in animal models with recognition of conspecifics. Functional MRI (fMRI) activation of CA2, CA3, and dentate gyrus has been described in learning (encoding) names of new faces (42, 43). In addition, one study demonstrated that anterior CA2 is used for learning the names and posterior is used for recall (retrieval) (43). Through disorders, such as prosopagnosia, we know that the fusiform gyrus is involved in face recognition, but there could be a network including CA2 and fusiform gyrus.

Limitations of the current study include the paucity of cognitive data, and the imbalance of sample sizes between the PART and ADNC groups, however the clinical and histologic data derived from the smaller number of ADNC cases is consistent with previously published reports on AD. In addition, since the study was designed to include a large number of total cases, only frontal and hippocampal sections were reevaluated for each case, precluding complete reassessment of Braak staging as this would require tau-stained sections of additional brain regions.

In conclusion, PART displays a predilection for CA2 neurofibrillary degeneration, which may be an aging process that is distinct from AD and independent of amyloid pathology, whereas significant CA1 neurofibrillary degeneration in the presence of amyloid plaques may be the initial dementia causing pathologic change in AD. Of course, more often than not, there are comorbidities, such as cerebrovascular disease, limbic predominant age-related TDP-43 encephalopathy (LATE), and LBD that may affect cognitive function. However, when only taking neurofibrillary degeneration into account, it appears that the path toward CA2 may be more benign. In future studies, it would be of interest to investigate the presence of comorbidities in PART, such as AGD, ARTAG, CTE, LATE, LBD, and cerebrovascular disease, and how the presence of these affect cognition. In addition, it is imperative that we develop a better understanding of the role of CA2 and the effect of pathology in the CA2 subregion as they relate to cognition and prognosis.

ACKNOWLEDGMENTS

The authors would like to thank Allison Beller and Kim Howard at University of Washington, Jeff Harris at UTSW, The Betty Martz Laboratory for Neurodegenerative Research, UCSD Alzheimer Disease Research Center personnel, The Neuropathology Core of the Massachusetts Alzheimer Disease Research Center, Ryan Cassidy Bohannan and Chad Caraway at the UCI Brain Repository, and the Neuropathology Brain Bank & Research CoRE at Mount Sinai. The Newcastle Brain Tissue Resource is funded in part by a grant from the UK Medical Research Council (G0400074), by Brains for Dementia research, a joint venture between Alzheimer's Society and Alzheimer's Research UK, and by the NIHR Newcastle Biomedical Research Centre awarded to the Newcastle upon Tyne Hospitals NHS Foundation Trust and Newcastle University. We acknowledge support from the Nancy and Buster Alvord Endowment, the J.M.R. Barker Foundation, the University of Texas Science and Technology Acquisition and Retention program award, and the Glenn Biggs Institute for Alzheimer's and Neurodegenerative Diseases at the Joe and Teresa Long School of Medicine, University of Texas Health Sciences Center, San Antonio, TX. In addition, the authors would also like to thank all of the brain donors for allowing this work to be possible.

REFERENCES

1. Bancher C, Jellinger KA. Neurofibrillary tangle predominant form of senile dementia of Alzheimer type: A rare subtype in very old subjects. Acta Neuropathol 1994;88:565–70

2. Jellinger KA, Attems J. Neurofibrillary tangle-predominant dementia: Comparison with classical Alzheimer disease. Acta Neuropathol 2007; 113:107–17
3. Jellinger KA, Bancher C. Senile dementia with tangles (tangle predominant form of senile dementia). Brain Pathol 2006;8:367–76
4. Crary JF. Primary age-related tauopathy and the amyloid cascade hypothesis: The exception that proves the rule? J Neurol Neuromedicine 2016;1:53–7
5. Montine TJ, Phelps CH, Beach TG, et al. National Institute on Aging-Alzheimer's Association guidelines for the neuropathologic assessment of Alzheimer's disease: A practical approach. Acta Neuropathol 2012; 123:1–11
6. Braak H, Braak E. Neuropathological stageing of Alzheimer-related changes. Acta Neuropathol 1991;82:239–59
7. Braak H, Braak E, Bohl J. Staging of Alzheimer-related cortical destruction. Eur Neurol 1993;33:403–8
8. Braak H, Del Tredici K. The pathological process underlying Alzheimer's disease in individuals under thirty. Acta Neuropathol 2011;121: 171–81
9. Braak H, Del Tredici K. From the entorhinal region via the prosubiculum to the dentate fascia: Alzheimer disease-related neurofibrillary changes in the temporal allocortex. J Neuropathol Exp Neurol 2020;79:163–75
10. Duyckaerts C, Delatour B, Potier MC. Classification and basic pathology of Alzheimer disease. Acta Neuropathol 2009;118:5–36
11. Crary JF, Trojanowski JQ, Schneider JA, et al. Primary age-related tauopathy (PART): A common pathology associated with human aging. Acta Neuropathol 2014;128:755–66
12. Braak H, Thal DR, Ghebremedhin E, et al. Stages of the pathologic process in Alzheimer disease: Age categories from 1 to 100 years. J Neuropathol Exp Neurol 2011;70:960–9
13. von Gunten A, Ebbing K, Imhof A, et al. Brain aging in the oldest-old. Curr Gerontol Geriatr Res 2010;2010:1–10.
14. Jellinger KA, Alafuzoff I, Attems J, et al. PART, a distinct tauopathy, different from classical sporadic Alzheimer disease. Acta Neuropathol 2015;129:757–62
15. Braak H, Del Tredici K. Are cases with tau pathology occurring in the absence of Abeta deposits part of the AD-related pathological process? Acta Neuropathol 2014;128:767–72
16. Duyckaerts C, Braak H, Brion JP, et al. PART is part of Alzheimer disease. Acta Neuropathol 2015;129:749–56
17. Ball MJ. Topographic distribution of neurofibrillary tangles and granulovacuolar degeneration in hippocampal cortex of aging and demented patients. A quantitative study. Acta Neuropathol 1978;42:73–80
18. Ball MJ. Neuronal loss, neurofibrillary tangles and granulovacuolar degeneration in the hippocampus with ageing and dementia. A quantitative study. Acta Neuropathol 1977;37:111–8
19. Milenkovic I, Petrov T, Kovacs GG. Patterns of hippocampal tau pathology differentiate neurodegenerative dementias. Dement Geriatr Cogn Disord 2014;38:375–88
20. Ball MJ. Topography of Pick inclusion bodies in hippocampi of demented patients. A quantitative study. J Neuropathol Exp Neurol 1979; 38:614–20
21. McKee AC, Stein TD, Kiernan PT, et al. The neuropathology of chronic traumatic encephalopathy. Brain Pathol 2015;25:350–64
22. Ishizawa T, Ko LW, Cookson N, et al. Selective neurofibrillary degeneration of the hippocampal CA2 sector is associated with four-repeat tauopathies. J Neuropathol Exp Neurol 2002;61:1040–7
23. Braak H, Del Tredici K, Rub U, et al. Staging of brain pathology related to sporadic Parkinson's disease. Neurobiol Aging 2003;24:197–211
24. Outeiro TF, Koss DJ, Erskine D, et al. Dementia with Lewy bodies: An update and outlook. Mol Neurodegener 2019;14:5
25. Butler TR, Self RL, Smith KJ, et al. Selective vulnerability of hippocampal cornu ammonis 1 pyramidal cells to excitotoxic insult is associated with the expression of polyamine-sensitive N-methyl-D-asparate-type glutamate receptors. Neuroscience 2010;165:525–34
26. Hatanpaa KJ, Raisanen JM, Herndon E, et al. Hippocampal sclerosis in dementia, epilepsy, and ischemic injury: Differential vulnerability of hippocampal subfields. J Neuropathol Exp Neurol 2014;73:136–42
27. Miyata H, Hori T, Vinters HV. Surgical pathology of epilepsy-associated non-neoplastic cerebral lesions: A brief introduction with special reference to hippocampal sclerosis and focal cortical dysplasia. Neuropathology 2013;33:442–58
28. Nelson PT, Dickson DW, Trojanowski JQ, et al. Limbic-predominant age-related TDP-43 encephalopathy (LATE): Consensus working group report. Brain 2019;142:1503–27
29. Nelson PT, Schmitt FA, Lin Y, et al. Hippocampal sclerosis in advanced age: Clinical and pathological features. Brain 2011;134:1506–18
30. Duvernoy H, Cattin F, Risold P-Y. Sectional anatomy and magnetic resonance imaging. In: Duvernoy H, Cattin F, Risold P-Y, eds. *The human hippocampus: Functional anatomy, vascularization and serial sections with MRI*. 4th ed. Heidelberg, Germany: Springer-Verlag 2013:129.
31. Mirra SS. The CERAD neuropathology protocol and consensus recommendations for the postmortem diagnosis of Alzheimer's disease: A commentary. Neurobiol Aging 1997;18:S91–4
32. Thal DR, Rub U, Orantes M, et al. Phases of A beta-deposition in the human brain and its relevance for the development of AD. Neurology 2002; 58:1791–800
33. Braak H, Braak E, Yilmazer D, et al. Functional anatomy of human hippocampal formation and related structures. J Child Neurol 1996;11: 265–75
34. Walker J, Richardson T, Farrell K, et al. Quantification and distribution of neuropathologic changes in primary age-related tauopathy. J Neuropathol Exp Neurol 2018;77:484.
35. Jellinger KA. Different patterns of hippocampal tau pathology in Alzheimer's disease and PART. Acta Neuropathol 2018;136:811–3
36. Jellinger KA. Primary age-related tauopathy (PART) and Alzheimer's disease (AD). Alzheimers Dement 2019;15:720
37. La C, Linortner P, Bernstein JD, et al. Hippocampal CA1 subfield predicts episodic memory impairment in Parkinson's disease. Neuroimage Clin 2019;23:101824
38. Adamowicz DH, Roy S, Salmon DP, et al. Hippocampal alpha-synuclein in dementia with Lewy bodies contributes to memory impairment and is consistent with spread of pathology. J Neurosci 2017;37:1675–84
39. Teylan M, Mock C, Gauthreaux K, et al. Cognitive trajectory in mild cognitive impairment due to primary age-related tauopathy. Brain 2020; 143:611–21
40. Chevaleyre V, Piskorowski RA. Hippocampal area CA2: An overlooked but promising therapeutic target. Trends Mol Med 2016;22:645–55
41. Hitti FL, Siegelbaum SA. The hippocampal CA2 region is essential for social memory. Nature 2014;508:88–92
42. Zeineh MM, Engel SA, Thompson PM, et al. Dynamics of the hippocampus during encoding and retrieval of face-name pairs. Science 2003;299: 577–80
43. Suthana NA, Donix M, Wozny DR, et al. High-resolution 7T fMRI of human hippocampal subfields during associative learning. J Cogn Neurosci 2015;27:1194–206